Int. J. Electron. Commun. (AEÜ) 99 (2019) 139–145

Contents lists available at ScienceDirect

International Journal of Electronics and Communications (AEÜ)

journal homepage: www.elsevier.com/locate/aeue

Regular paper

Efficient DOA estimation based on difference-set table traversal searching for the generalized coprime array

Xiang-Dong Huang [a], Jing-Wen Xu [a], Tian-Lei Nian [b], Qian Lin [b,*]

[a] School of Electrical and Information Engineering, Tianjin University, Tianjin, China
[b] College of Physics and Electronic Information Engineer, Qinghai Nationalities University, Xining, China

ARTICLE INFO

Article history:
Received 6 March 2018
Accepted 14 November 2018

Keywords:
DOA estimation
Difference-set table
Generalized coprime array
Virtual Nyquist-ULA

ABSTRACT

This paper aims to achieve both high degree-of-freedom (DOF) and high efficiency in direction-of-arrival (DOA) estimation. On one hand, to realize high DOF, this paper optimizes the interelement spacings and the displacement of the generalized coprime sparse array. On the other hand, to achieve high efficiency, a series of approaches are proposed: Firstly, a normalized-coordinate representation is formulated to explore the conversion relationship between the covariance matrix of the physical sparse array and that of the expected virtual Nyquist uniform linear array (ULA); Secondly, a difference-set table traversal searching method is proposed to guide this conversion; Thirdly, the mapping relationship between the element coordinates in the observation covariance matrix and a lag of the Nyquist-ULA is built up, from which the DOAs can be readily estimated through MUSIC decomposition. Deep analysis shows that the proposed estimator saves approximately $O((MN+1)^3)$ times of multiplications involved in the spatial smoothing based estimator. Numerical results also confirmed that our proposed estimator does not pay the cost of performance attenuation, which presents vast potentials in radar, communication and sonar systems, etc.

1. Introduction

In recent years, the sparse array, whose interelement spacings allow to be greater than the half wavelength of the incident signal, has become a hot topic in the field of array signal processing [1]. Especially, direction-of-arrival (DOA) estimation [2] based on sparse arrays, which is able to realize high degrees-of-freedom (DOF) only consuming a small quantity of sensors, receives increasing attention [3–9]. Generally speaking, a sparse array's DOF depends on the number of consecutive lags by enumerating all possible differences of the sensor locations, which is essentially determined by this sparse array's structure [10,11].

A number of sparse array structures, each of which usually consists of two uniform linear subarrays (ULAs), have been proposed to realize higher DOFs using finite number of sensors [12]. For example, the nested arrays [3,4], are able to resolve up to $O(N^2)$ sources with $O(N)$ sensors. Another typical example is the prototype coprime array [5], which is composed up of an M-sensor subarray with an interelement spacing of N half-wavelengths and an N-sensor subarray with an interelement spacing of M half-wavelengths (M, N are a pair of coprime integers). This array can resolve $O(MN)$ sources with $M+N-1$ sensors; Following this, an extended coprime array was proposed in [6]. By means of increasing the element number of a subarray (from M to $2M$, i.e., the total sensor number is $N+2M-1$), the correlation lag of this sparse array continuously ranges from $-MN$ to MN. To further cut down the hardware cost, a generalized *coprime array with displaced subarrays* (CADiS) was devised in [7], which only consumes $N+M-1$ sensors to realize the same DOF of the extended coprime array. In other words, the ratio of DOF to the sensor number is greatly enhanced, thus this generalized coprime sparse array may be the most fascinating sparse array.

Practically, once a sparse array structure is determined, it is expected that DOA estimation be implemented in an efficient way. However, the DOA estimation addressed in [7] experiences a process of spatial smoothing [13–15] (see Section 3.4 for details), which consumes heavy computational complexity. If spatial smoothing can be omitted, the efficiency of DOA estimation will be undoubtedly enhanced.

This paper proposes an efficient DOA estimator for the CADiS sparse array. By formulating a normalized-coordinate representation of the covariance matrix, we build up a conceptual relationship between the physical CADiS sparse array and the virtual

* Corresponding author.
E-mail addresses: xdhuang@tju.edu.cn (X.-D. Huang), linqian@tju.edu.cn (Q. Lin).

https://doi.org/10.1016/j.aeue.2018.11.028
1434-8411/

Nyquist-ULA. On basis of this relationship, a difference-set table traversal searching method is developed. This method plays the role of guiding a conversion from the physical array's covariance matrix to the virtual Nyquist-ULA's covariance matrix, from which DOAs can be directly estimated through MUSIC decomposition. Due to the fact that spatial smoothing is not involved in the above dataflow, our proposed estimator behaves more efficient than the estimator in [7]. Moreover, numerical results also confirmed a consistency between these two estimators' spatial spectra, indicating that the efficiency enhancement of our proposed estimator does not pay the cost of performance degradation.

Notations: we use boldface uppercase letters to denote matrices, boldface lowercase letters for column vectors. $\mathbf{I}$ denotes the identity matrix. $(\cdot)^{\mathrm{T}}$ and $(\cdot)^{\mathrm{H}}$ respectively denote the transpose and conjugate transpose of a vector or matrix.

2. System model

2.1. Normalized-coordinate representation of covariance matrix

Consider a radar system with the wavelength λ, in which a linear array with L sensors is deployed to detect Q narrowband far-field sources $s_1,\ldots,s_Q$ from directions $\theta_1,\ldots,\theta_Q$. To emphasize, no restriction is imposed on the interelement spacings $d_l, l=1,\ldots,L-1$, between adjacent sensors. In other words, this array allows to be an Nyquist-ULA (i.e., $d_l=\frac{\lambda}{2}, l=1,\ldots,L-1$) or a sparse array (i.e., $d_l=\frac{n\lambda}{2}, n\in\mathbf{Z}^+$ ($\mathbf{Z}^+$ refers to the positive integer set)).

Clearly, the coordinate of the l-th sensor referenced to the 0-th sensor is

$$D_l=\begin{cases}0, & l=0,\\ \sum_{j=1}^{l} d_j, & l=1,\ldots,L-1.\end{cases} \tag{1}$$

As is known, the L-length receiver vector $\boldsymbol{x}=[x_0,x_1,\ldots,x_{L-1}]^{\mathrm{T}}$ is formulated as [7]

$$\boldsymbol{x}=\sum_{q=1}^{Q}\boldsymbol{a}(\theta_q)s_q+\boldsymbol{n}=\boldsymbol{A}\boldsymbol{s}+\boldsymbol{n}, \tag{2}$$

where

$$\boldsymbol{a}(\theta_q)=\left[1,e^{-\mathrm{j}\pi\frac{D_1}{\lambda/2}\sin\theta_q},\ldots,e^{-\mathrm{j}\pi\frac{D_{L-1}}{\lambda/2}\sin\theta_q}\right]^{\mathrm{T}}, \tag{3}$$

$$\boldsymbol{A}=[\boldsymbol{a}(\theta_1),\ldots,\boldsymbol{a}(\theta_Q)], \tag{4}$$

$$\boldsymbol{s}=[s_1,\ldots,s_Q]^{\mathrm{T}}, \tag{5}$$

refer to the steering vector of the incident angle θ_q, the array manifold matrix, and the source vector, respectively. The noise $\boldsymbol{n}$ is assumed to be temporally and spatially white, and uncorrelated from the sources, whose variance is σ_n^2.

On basis of (2)–(5), the observation covariance matrix $\hat{\boldsymbol{\Phi}}$ can also be formulated as

$$\hat{\boldsymbol{\Phi}}=\mathrm{E}[\boldsymbol{x}\boldsymbol{x}^{\mathrm{H}}]=\sum_{q=1}^{Q}\sigma_q^2\boldsymbol{a}(\theta_q)\boldsymbol{a}^{\mathrm{H}}(\theta_q)+\sigma_n^2\mathbf{I}, \tag{6}$$

where $\sigma_1^2,\ldots,\sigma_Q^2$ are the powers of sources $s_1,..,s_Q$.

Further, we normalize the coordinates of these L sensors using the half wavelength as

$$c_l=\frac{D_l}{\lambda/2},\quad l=0,\ldots,L-1. \tag{7}$$

Substituting (7) into (3) yields

$$\boldsymbol{a}(\theta_q)=[1,e^{-\mathrm{j}\pi c_1\sin\theta_q},\ldots,e^{-\mathrm{j}\pi c_{L-1}\sin\theta_q}]^{\mathrm{T}}. \tag{8}$$

Denote an $L\times L$ matrix $\boldsymbol{\Psi}_q$ as

$$\boldsymbol{\Psi}_q=\boldsymbol{a}(\theta_q)\boldsymbol{a}^{\mathrm{H}}(\theta_q). \tag{9}$$

Thus we have

$$\hat{\boldsymbol{\Phi}}=\sum_{q=1}^{Q}\sigma_q^2\boldsymbol{\Psi}_q+\sigma_n^2\mathbf{I}. \tag{10}$$

Combining (8) with (9), one can derive its inner elements

$$\psi_q(u,v)=e^{-\mathrm{j}\pi(c_u-c_v)\sin\theta_q},\quad u,v=0,\ldots,L-1. \tag{11}$$

The inner elements of $\hat{\boldsymbol{\Phi}}$ can be derived from (9)–(11) as

$$\hat{\phi}(u,v)=\begin{cases}\sigma_n^2+\sum_{q=1}^{Q}\sigma_q^2, & u=v\\ \sum_{q=1}^{Q}\sigma_q^2e^{-\mathrm{j}\pi(c_u-c_v)\sin\theta_q}, & u\neq v\end{cases}. \tag{12}$$

From the physical interpretation, $\hat{\phi}(u,v)$ stands for the cross-correlation between the u-th sensor and the v-th sensor, i.e.,

$$\hat{\phi}(u,v)=\frac{1}{K}\sum_{n=0}^{K-1}x_u(n)x_v(n), \tag{13}$$

where $x_u(n)$, $x_v(n)$ refer to the snapshots recorded at two sensors and K is the snapshot number.

Further, notice that the covariance function $\hat{\phi}(u,v)$ in (12) heavily depends on c_u-c_v, i.e., the difference of two sensors' normalized coordinates. Thus it can be written as

$$\hat{\phi}(u,v)=\hat{\phi}_{c_u-c_v}. \tag{14}$$

As is known, only when a covariance matrix $\tilde{\boldsymbol{\Phi}}$ possesses a Toeplitz structure as

$$\tilde{\boldsymbol{\Phi}}=\begin{bmatrix}\hat{\phi}_0 & \hat{\phi}_{-1} & \cdots & \hat{\phi}_{-\tilde{L}+1}\\ \hat{\phi}_1 & \hat{\phi}_0 & \cdots & \hat{\phi}_{-\tilde{L}+2}\\ \vdots & \vdots & \ddots & \vdots\\ \hat{\phi}_{\tilde{L}-1} & \hat{\phi}_{\tilde{L}-2} & \cdots & \hat{\phi}_0\end{bmatrix} \tag{15}$$

and its adjacent inner element pairs satisfy

$$\hat{\phi}_l/\hat{\phi}_{l-1}=\text{constant},\quad l\in[-\tilde{L}+2,\tilde{L}-1], \tag{16}$$

can DOAs be estimated from MUSIC decomposition [16].

Eqs. (14) and (16) indicate that, the construction of the expected covariance matrix $\tilde{\boldsymbol{\Phi}}$ requires that the differences of normalized coordinates c_u-c_v be consecutive in the interval $[-\tilde{L}+1,\tilde{L}-1]$. This requirement helps to explore a relationship between the observation covariance matrix $\hat{\boldsymbol{\Phi}}$ and the expected covariance matrix $\tilde{\boldsymbol{\Phi}}$, and this relationship will be discussed for the Nyquist-ULA case and the sparse array case, respectively.

2.2. Relationship of covariance matrices for the Nyquist-ULA

For the case of Nyquist dense array (i.e., $D_l=\frac{\lambda}{2}l$), we have

$$c_l=l,\quad l=0,\ldots,L-1. \tag{17}$$

Substituting (17) into (14), we have

$$\hat{\phi}(u,v)=\hat{\phi}_{c_u-c_v}=\hat{\phi}_{u-v}. \tag{18}$$

Clearly, for all integers $u,v\in[0,L-1]$, the difference c_u-c_v (i.e., $u-v$) traverses all $2L-1$ consecutive integers in $[-L+1,L-1]$. Hence, combining (15) and (16) with (18), we have

$$\tilde{L} = L, \quad \tilde{\mathbf{\Phi}} = \hat{\mathbf{\Phi}}, \tag{19}$$

i.e., the expected covariance matrix $\tilde{\mathbf{\Phi}}$ is exactly the observation covariance matrix $\hat{\mathbf{\Phi}}$.

2.3. Relationship of covariance matrices for a sparse array

The significance of a sparse array lies in identifying more objects (i.e., increasing the DOF) than the Nyquist array with the same sensor number does. Accordingly, the consecutive range $[-\tilde{L}+1, \tilde{L}-1]$ traversed by its normalized coordinate difference $c_u - c_v$ should be wider than that of the Nyquist array $[-L+1, L-1]$ (i.e., $\tilde{L} > L$ and thus the size of $\tilde{\mathbf{\Phi}}$ is larger than that of $\hat{\mathbf{\Phi}}$).

However, for a sparse array, since its interelement spacing d_l allows to be multiple times of the half wavelength, its normalized coordinate $c_l \neq l$. This may result in that, if the structure of the sparse array is not properly devised, $c_u - c_v$ becomes inconsecutive in the expected range $[-\tilde{L}+1, \tilde{L}-1]$ (i.e., some holes occur in this interval).

Hence, in order to increase the DOF of a sparse array with L sensors, it is crucial to optimize the array structure such that the normalized coordinate differences $c_u - c_v$ $(u, v \in [0, L-1])$ are consecutive in a range as wide as possible (i.e., the ratio $\tilde{L}/L$ should be great as possible).

For this reason, we choose the generalized coprime array [7]. Furthermore, we propose a difference-set table traversal searching method, which greatly facilitates the guidance of the conversion from the observation covariance matrix to the expected covariance matrix (actually the covariance matrix of a virtual Nyquist-ULA with a larger aperture).

3. The proposed DOA estimator

3.1. Optimal parameterization on the generalized coprime array

The generalized coprime sparse array [7] is derived from the extended coprime sparse array [6]. Nevertheless, to obtain a maximum DOF for the generalized coprime sparse array, optimal parameterization needs to be done.

The structure of the extended coprime sparse array is characterized by interlacing the sensors of two sub-ULAs. As Fig. 1 illustrates, sub-ULA1 consists of N sensors located at $0, Md, \ldots, (N-1)Md$ $(d = \frac{\lambda}{2})$ whereas sub-ULA2 consists of $2M$ sensors located at $0, Nd, \ldots, (2M-1)Nd$ $(M < N)$. Thus, this array contains $L = N + 2M - 1$ sensors, whose normalized coordinates constitute the following set

$$\begin{aligned} \boldsymbol{C} &= \{nM, 0 \leqslant n \leqslant N-1\} \cup \{mN, 0 \leqslant m \leqslant 2M-1\} \\ &= \{c_0, c_1, \ldots, c_{L-1}\} \end{aligned}. \tag{20}$$

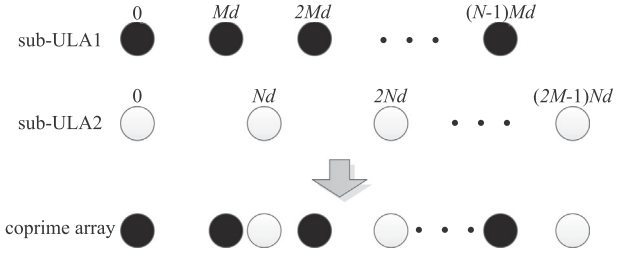

Fig. 1. The extended coprime array configuration.

To explain that the normalized coordinate differences $c_u - c_v$ $(u, v \in [0, L-1])$ are consecutive in the range $[-\tilde{L}+1, \tilde{L}-1]$ $(\tilde{L} = MN + M)$. Obviously, the coordinate difference set $\mathbf{T} = \{c_u - c_v, u, v \in [0, L-1]\}$ contains 4 cases: two self-difference sets $\mathbf{L}_{s1} = \{nM - n'M, 0 \leqslant n \leqslant N-1\}$ $\mathbf{L}_{s2} = \{mN - m'N, 0 \leqslant m \leqslant 2M-1\}$, and two cross-difference sets $\mathbf{L}_{c1} = \{nM - mN, 0 \leqslant n \leqslant N-1, 0 \leqslant m \leqslant 2M-1\}, \mathbf{L}_{c2} = \{mN - nM, 0 \leqslant n \leqslant N-1, 0 \leqslant m \leqslant 2M-1\}$ ($\mathbf{L}_{c1}$ and $\mathbf{L}_{c2}$ are symmetric). Thus, $\mathbf{T} = \mathbf{L}_{s1} \bigcup \mathbf{L}_{s2} \bigcup \mathbf{L}_{c1} \bigcup \mathbf{L}_{c2}$.

Clearly, once the conclusion that any $c \in [0, MN + M - 1]$ can be consecutively determined in the subset $\mathbf{L}_{c1}$ holds, we can also derive that $c \in [-MN - M + 1, MN + M - 1]$ can be consecutively determined in the overall coordinate difference set $\mathbf{T}$. This conclusion can be drawn from the following proposition, which is proved in Appendix A.

Proposition 1. *There exists a unique integer pair $(m, n), n \in [0, N-1], m \in [0, 2M-1]$, such that any integer $c \in [0, MN + M - 1]$ can be determined by the substraction $c = mN - nM$.*

On basis of the extended coprime sparse array, three improved measures were proposed to enhance the ability of detecting objects. Firstly, the sensor number of sub-ULA2 is reduced from $2M$ to $M-1$, thus the overall sensor number is reduced from $L = 2M + N - 1$ to $L = M + N - 1$; Secondly, the interelement spacing of sub-ULA1 is compressed from $M\frac{\lambda}{2}$ to $\tilde{M}\frac{\lambda}{2}$, where M can be divided by $\tilde{M}$ (i.e., $M = p\tilde{M}, p \in \mathbf{Z}^+$); Thirdly, the interlacing assembly mode of two sub-ULAs is replaced by the displacement mode. As Fig. 2 depicts, there exists a displacement of γd $(\gamma \in \mathbf{Z}^+)$ between these two sub-ULAs. Hence this improved array is called the generalized *coprime array with displaced subarrays*(CADiS) [7], whose normalized positions are formulated as

$$\begin{aligned} \boldsymbol{C} = \; & \{n\tilde{M}, 0 \leqslant n \leqslant N-1\} \cup \\ & \{\tilde{M}(N-1) + \gamma + mN, 0 \leqslant m \leqslant M-2\}. \end{aligned} \tag{21}$$

As [7] pointed out, when the normalized displacement $\gamma = \tilde{M} + N$, the number of consecutive lags of the generalized coprime array reaches the maximum $MN - (\tilde{M}-1)(N-2) + 1$.

Furthermore, for the sake of maximizing the DOF, we might as well specify $\tilde{M} = 1$, which results in that the number of consecutive lags is $MN + 1$. In other words, the normalized coordinate differences $c_u - c_v$ $(u, v \in [0, L-1])$ are consecutive in the range $[-\tilde{L}+1, \tilde{L}-1]$ $(\tilde{L} = MN + 1)$. Accordingly, substituting $\tilde{M} = 1, \gamma = N + 1$ into (21) yields

$$\boldsymbol{C} = \{0, 1, \ldots, N-1, 2N, 3N, \ldots, MN\}. \tag{22}$$

With the above optimal parameterization on the generalized coprime array, the ratio of $\tilde{L}/L$ increases from $\frac{MN+M}{2M+N-1}$ to $\frac{MN+1}{M+N-1}$ (since $MN + M \propto O(MN)$), meaning that this array is able to realize a high DOF with a low hardware cost.

3.2. DOA Estimation based on difference-set table traversal searching

Recall that, once the structure of a sparse array is chosen, the key is to convert the observation covariance matrix $\hat{\mathbf{\Phi}}$ to the larger-size Nyquist-ULA covariance matrix $\tilde{\mathbf{\Phi}}$.

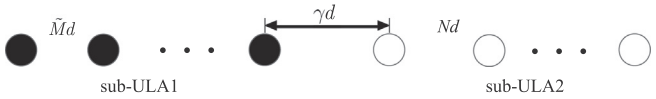

Fig. 2. The CADiS structure of the generalized coprime array.

As mentioned above, for the generalized coprime array with the parameterization $\tilde{M}=1$ and $\gamma=N+1, c_u-c_v$ is consecutive in the range $[-\tilde{L}+1,\tilde{L}-1]$ $(\tilde{L}=MN+1)$. In turn, for each $\hat{\phi}_l(l\in[-\tilde{L}+1,\tilde{L}-1])$ in the expected Nyquist covariance matrix $\tilde{\mathbf{\Phi}}$, it is certain that there exists at least one element $\hat{\phi}(u,v)$ in the observation covariance matrix $\hat{\mathbf{\Phi}}$ such that $c_u-c_v=l$.

Hence, it is necessary to create an $L\times L$-size difference-set table $\mathbf{T}$ to disclose the mapping relationship between the element coordinate (u,v) in the matrix $\hat{\mathbf{\Phi}}$ and the lag l involved in the matrix $\tilde{\mathbf{\Phi}}$. In other words, the inner elements $T(u,v)$ of this table are formulated as

$$T(u,v)=c_u-c_v,\quad u,v\in[0,L-1]. \tag{23}$$

Guided by this table, for each lag l, one can search out a coordinate set $P_l=\{(u,v)|c_u-c_v=l\}$ and then average all the elements inside P_l to acquire a more accurate covariance estimate as

$$\tilde{\phi}_l=\frac{1}{|P_l|}\sum_{(u,v)\in P_l}\hat{\phi}(u,v),\ l\in[-\tilde{L}+1,\tilde{L}-1]. \tag{24}$$

Further, substituting $\hat{\phi}_{-\tilde{L}+1},\ldots,\hat{\phi}_{\tilde{L}-1}$ in (15) with $\tilde{\phi}_{-\tilde{L}+1},\ldots,\tilde{\phi}_{\tilde{L}-1}$ in (24), one can obtain the expected covariance matrix $\tilde{\mathbf{\Phi}}$ of the virtual Nyquist-ULA as

$$\tilde{\mathbf{\Phi}}=\begin{bmatrix}\tilde{\phi}_0 & \tilde{\phi}_{-1} & \cdots & \tilde{\phi}_{-MN}\\ \tilde{\phi}_1 & \tilde{\phi}_0 & \cdots & \tilde{\phi}_{-MN+1}\\ \vdots & \vdots & \ddots & \vdots\\ \tilde{\phi}_{MN} & \tilde{\phi}_{MN-1} & \cdots & \tilde{\phi}_0\end{bmatrix}. \tag{25}$$

Then, implementing MUSIC decomposition on $\tilde{\mathbf{\Phi}}$ yields all the DOA estimates.

3.3. Estimator summary and complexity analysis

A 3-step procedure for the proposed DOA estimator is summarized in Table 1. Here we present a quantitative complexity analysis step by step, which is evaluated by the consumed times of multiplications.

In Step 1, by utilization of the snapshots collected at $N+M-1$ sensors, it can be inferred from (6) that the calculation of the observation covariance matrix $\hat{\mathbf{\Phi}}$ consumes $O(K(N+M-1)^2)$ multiplications.

Step 2 mainly aims to convert the observation covariance matrix $\hat{\mathbf{\Phi}}$ to the virtual Nyquist-ULA's covariance matrix $\tilde{\mathbf{\Phi}}$. One can discover that this step only involve several multiplication-free operations such as integer subtractions (to build up the difference-set table), table lookup operations and element arrangement operations.

Step 3 addresses the eigen-decomposition of an $(MN+1)\times(MN+1)$ matrix $\tilde{\Phi}$, which requires around $O((MN+1)^3)$ operations [17].

Table 1
Procedure of the proposed DOA estimator

Step 1	Calculate the observation covariance matrix $\hat{\mathbf{\Phi}}$ using all K snapshots collected at $L=M+N-1$ sensors of the generalized coprime array.
Step 2	Construct the L-length normalized coordinate set as $\boldsymbol{C}=\{0,1,\ldots,N-1,2N,3N,\ldots,MN\}$ and create an $L\times L$-size difference-set table $\mathbf{T}$ in terms of (23). Let $\tilde{L}=MN+1$. For each lag $l\in[-\tilde{L}+1,\tilde{L}-1]$, search out all the coordinates (u,v) in the table $\mathbf{T}$ such that $c_u-c_v=l$ and substitute (u,v) into (24) to calculate $\tilde{\phi}_l$ in the expected covariance matrix $\tilde{\mathbf{\Phi}}$.
Step 3	Implementing MUSIC decomposition on $\tilde{\mathbf{\Phi}}$ yields all the DOA estimates.

Overall, $O(K(N+M-1)^2)+O((MN+1)^3)$ times of multiplications are consumed.

3.4. Comparison analysis for complexity

The DOA estimator in [7] also needs the calculation of the observation covariance matrix (in Step 1) and MUSIC decomposition (in Step 3). The difference between the DOA estimator in [7] and the proposed estimator lies in that, the conversion from $\hat{\mathbf{\Phi}}$ to $\tilde{\mathbf{\Phi}}$ (i.e., Step 2) is much more complex.

For the DOA estimator in [7], this conversion experiences the following steps: Firstly, vectorize the matrix $\hat{\mathbf{\Phi}}$ to generate an L^2-length vector $\mathbf{z}$; Secondly, extract all the consecutive lag samples of $\mathbf{z}$ and form a new $\mathbf{z}_1$; Thirdly, divide $\mathbf{z}_1$ into $MN+1$ overlapping subarrays $\mathbf{z}_{1,i}, i=1,\ldots,MN+1$; Fourthly, for $i=1,\ldots,MN+1$, construct sub-covariance matrices $\mathbf{R}_i=\mathbf{z}_{1,i}\mathbf{z}_{1,i}^{\mathrm{H}}$ (each matrix $\mathbf{R}_i$ is of the size $(MN+1)\times(MN+1)$); Lastly, averaging $\mathbf{R}_1,\ldots,\mathbf{R}_{MN+1}$ yields the final covariance matrix $\tilde{\mathbf{\Phi}}$. The above 5-step conversion is also called the *spatial smoothing* operation [7].

Obviously, the computation complexity of the above 5-step spatial smoothing operation mainly focuses on the fourth step. Specifically, calculation of each sub matrix $\mathbf{R}_i$ consumes $O((MN+1)^2)$ times of complex multiplications. As a result, calculation of $\mathbf{R}_1,\ldots,\mathbf{R}_{MN+1}$ consumes $O((MN+1)^3)$ times of complex multiplications [18].

Overall, the DOA estimator in [7] consumes $O(K(N+M-1)^2)+O((MN+1)^3)+O((MN+1)^3)$ times of multiplications.

Since $O((MN+1)^3)$ times of complex multiplications are saved, the proposed DOA estimator is more efficient.

One can notice that, both our proposed estimator and the spatial smoothing based estimator in [7] involve the averaging operation. Specifically, the former averaging operation is implemented on those corresponding matrix elements guided by the coordinate difference set, whereas the latter averaging operation is implemented on $(MN+1)\times(MN+1)$-sized sub-covariance matrices $\mathbf{R}_1,\ldots,\mathbf{R}_{MN+1}$. Essentially, for the latter estimator, the generation of $\mathbf{R}_i=\mathbf{z}_{1,i}\mathbf{z}_{1,i}^{\mathrm{H}}$ also incorporates the coordinate difference operation. In combination with the fact that both estimators stem from a common observation covariance matrix $\hat{\mathbf{\Phi}}$, both estimators are essentially equivalent (besides, our proposed estimator is more efficient) and they surely lead to the same result, which will be verified by means of numerical simulations.

4. Numerical results and analysis

4.1. Demonstration of the difference-set table guidance

Consider that $Q=3$ far-field narrowband sources with the incident directions $[\theta_1,\theta_2,\theta_3]=[20^\circ,50^\circ,58^\circ]$ are impinging on two arrays with the same 4 sensors. One is the generalized coprime sparse array with $M=3,N=2$ (thus $L=N+M-1=4$ and $\tilde{L}=MN+1=7$); The other is the conventional dense Nyquist-ULA. For both arrays, $K=3000$ snapshots are collected at each sensor and the signal-to-noise ratio (SNR) is set as 0 dB. The proposed method and the conventional MUSIC method are respectively employed to estimate 3 DOAs of these two arrays.

For the proposed method, following Step 1-Step 2 listed in Table 1, one can construct the normalized coordinate set $\boldsymbol{C}=\{0,1,4,6\}$, whose differences $T(u,v)=c_u-c_v, u,v=0,\ldots,3$, are listed in Table 2. Guided by this difference-set Table, the mapping relationship between the corresponding coordinates (u,v) in the observation covariance matrix $\hat{\mathbf{\Phi}}$ and the lags $l\in[-\tilde{L}+1,\tilde{L}-1]=[-6,6]$ is reflected in Table 3. Then, following Step 2 and

Table 2
The difference-set table ($M = 3, N = 2$).

$T(u, v)$	$v = 0$	$v = 1$	$v = 2$	$v = 3$
$u = 0$	0	−1	−4	−6
$u = 1$	1	0	−3	−5
$u = 2$	4	3	0	−2
$u = 3$	6	5	2	0

Step 3, we acquire the spatial spectrum plotted in Fig.3(a). Besides, as a reference, Fig. 3(b) also illustrates the spatial spectrum for the Nyquist-ULA.

One can notice that, the resolution of the spatial spectrum in Fig. 3(a) is higher than that of the spatial spectrum in Fig. 3(b), since the former spectrum can discriminate two densely located directions $[\theta_2, \theta_3] = [50^\circ, 58^\circ]$ while the latter cannot. This attributes from the advantage that, the CADiS is a sparse array, and it can be converted into a virtual Nyquist-ULA by means of the proposed difference-set table traversal searching method. This conversion actually widens the array aperture (from $L = 4$ to $\tilde{L} = 7$), thereby enhancing the spatial resolution.

4.2. Performance comparison with the spatial smoothing method

Consider the same CADiS with $M = 4, N = 3$ (thus $L = N + M - 1 = 6$ and $\tilde{L} = MN + 1 = 13$); Assume that there are $Q = 12$ far-field narrowband sources with the incident directions uniformly located in the range $[-60^\circ, 50^\circ]$ impinging on this generalized coprime sparse array. The snapshot number and the SNR condition are same as Section 4.1. Fig. 4 illustrates the spatial spectra resulting from the proposed estimator (marked in "∘") and the spatial smoothing based estimator in [7] (marked in "∗"), respectively.

As Fig. 4 depicts, these two spatial spectra fully overlap and their detected DOAs are uniformly located in the range $[-60^\circ, 50^\circ]$, thereby confirming the aforementioned equivalence between two estimators. Nevertheless, recall that, when dealing with the core part —— the conversion of covariance.

4.3. Comparisons of accuracy, robustness and efficiency

This subsection aims to compare the root mean squared error (RMSE) of the DOA estimation among the proposed estimator, the spatial-smoothing based estimator and the Nyquist-ULA based estimator.

For all estimators, the sensor number is set as $L = 6$, requiring that the CADiS array parameters be set as $M = 4,\ N = 3$ (thus $N + M - 1 = 6$). To well reflect the anti-noise robustness and accuracy, only $Q = 1$ far-field narrowband source with the incident direction $\theta = 45^\circ$ was considered (Snapshot number $K = 1000$). SNR varies in a region $[-20\ dB, 25\ dB]$. For each SNR case and each estimator, 1000 Monte Carlo trials were conducted. Fig. 5 illustrates the RMSE curves of 3 estimators, from which the following conclusions can be drawn.

(1) The RMSE curve of the proposed estimator (marked in "∘") is located below that of the Nyquist-ULA based estimator (marked in "◇"). In other words, the proposed estimator achieves higher accuracy. This attributes to the fact that, given the same sensor number, the sparse array actually obtains a larger aperture than the Nyquist-ULA does.
(2) In the low SNR region, all 3 estimators consistently have the same SNR threshold −16 dB (below which an estimator falls failure), indicating that they almost obtain the same anti-noise robustness.
(3) The RMSE curves of the proposed estimator and the spatial-smoothing based estimator (marked in "∗") fully overlap, which also reflecting the equivalence between two estimators. Nevertheless, as aforementioned, our proposed estimator's calculation efficiency is higher than the latter.

Further, we used the algorithm execution time (200 runs of algorithm implementation) to compare these two estimators' calculation efficiency. Their related parameters were set as follows: $M = 11,\ N = 13$, the snapshot number $K = 1000$; Both algorithms were running on the same software MATLAB R2016b platform: Windows 10 (pro) workstation with a Intel Core i5 2.60 GHz CPU and 8 GB RAM. Our experimental results showed that, the

Table 3
Mapping relationship between the coordinates and the lags.

l	−6	−5	−4	−3	−2	−1	
$\{(u, v)\}$	(0,3)	(1,3)	(0,2)	(1,2)	(2,3)	(0,1)	
l	0	1	2	3	4	5	6
$\{(u, v)\}$	(0,0), (1,1), (2,2), (3,3)	(1,0)	(3,2)	(2,1)	(2,0)	(3,1)	(3,0)

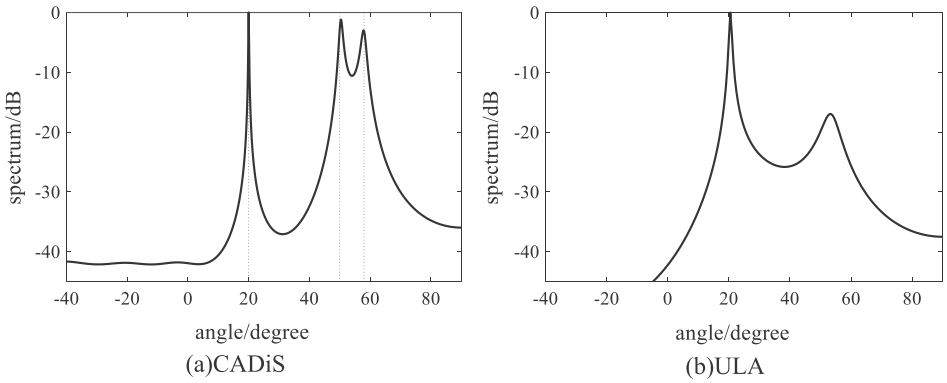

Fig. 3. Spatial spectra estimated using MUSIC for two methods ($M = 3, N = 2, \tilde{M} = 1$). (a) Proposed method based on CADiS. (b) MUSIC method based on Nyquist-ULA.

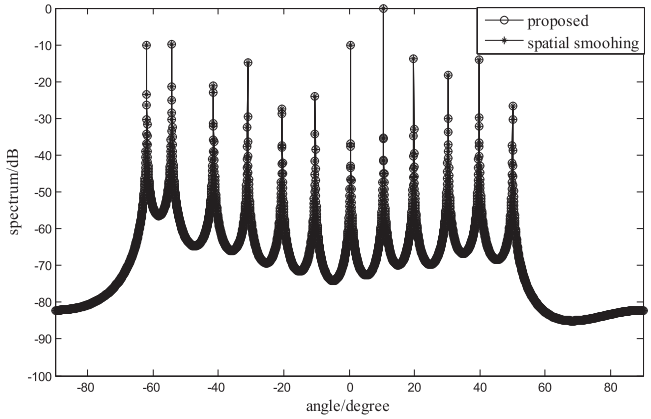

Fig. 4. Spatial spectra estimated of two methods.

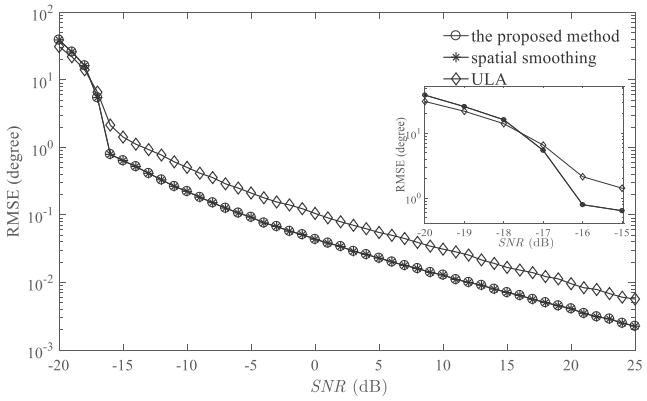

Fig. 5. RMSE versus SNR.

spatial-smoothing based estimator took 44.5270 s, whereas the proposed estimator spent 33.3863 s (i.e., 25.02% reduction).

4.4. Comparison with the compressive sensing based estimator

The Compressive Sensing (CS) Estimator for the CADiS array in [7] is based on the following optimization

$$\hat{\mathbf{r}}^{o} = \arg\min_{\mathbf{r}^{o}} \left[\frac{1}{2} \left\| \mathbf{z} - \mathbf{B}^{o}\mathbf{r}^{o} \right\|_2 + \lambda_t \left\| \mathbf{r}^{o} \right\|_1 \right], \tag{26}$$

where $\mathbf{z}$ is of the size $(M+N-1)^2 \times 1$ derived by vectorizing the observation covariance matrix $\hat{\mathbf{\Phi}}$, $\mathbf{B}^{o}$ actually refers to a dictionary consisting self-Kronecker-producted steering vectors for a mass of candidate DOAs, and $\mathbf{r}^{o}$ refers to the power of the target in the direction of a candidate DOA. Besides, λ_t is a penalty parameter which can be tuned to trade off the error of the number of nonzero entries (degree of sparsity) in the estimates [7]. The proposed estimator is more practical than the CS-based estimator, which is drawn from the following two aspects of simulation results: (1) As Fig. 6 depicts, the proposed estimator behaves more stable than the CS based estimator does, since the former is a parameter-free estimator whereas the latter is a parameter-dependant one.

Table 4
Comparison of consumed execution time.

Scanning step	0.025°	0.05°	0.25°	0.5°	1°
Proposed	0.01(s)	0.009(s)	0.008(s)	0.006(s)	0.006(s)
CS-based	292.24(s)	71.81(s)	3.13(s)	2.675(s)	2.379(s)

Specifically, the DOAs detected by the proposed estimator exactly fall at the ideal positions $20°, 50°, 58°$, and the out-of-band attenuation reaches about -41 dB. In contrast, the performance of the CS-based estimator heavily relies on the parameter λ_t . For the case $\lambda_t = 32$, although the out-of-band attenuation reaches about -98 dB, the detected DOAs seriously deviated from these ideal positions (e.g., the detection error corresponding to the DOA $58°$ reaches $3°$). For the case $\lambda_t = 15$, although the detected DOAs approximate these ideal positions, the out-of-band attenuation is only about -28 dB.

(2) As Table 4 lists, no matter what the angle scanning step is chosen, the proposed estimator behaves much more efficient than the CS-based estimator, since the execution time consumed by the former estimator is generally much shorter than that of the latter estimator.

This computation superiority lies in: our proposed estimator only involves simple difference-set table based covariance matrix conversion and MUSIC decomposition, compared to that the CS-based estimator involves the construction of a redundant dictionary, the tedious matching pursuit for dictionary entries and other optimization operations.

5. Conclusion

This paper proposes an efficient DOA estimator based on difference-set table searching for the generalized coprime array. The high efficiency lies in that, the proposed difference-set table searching method well guides the conversion from the observation covariance matrix to the virtual Nyquist-ULA's covariance matrix, which saves $O((MN+1)^3)$ times of multiplication involved in the

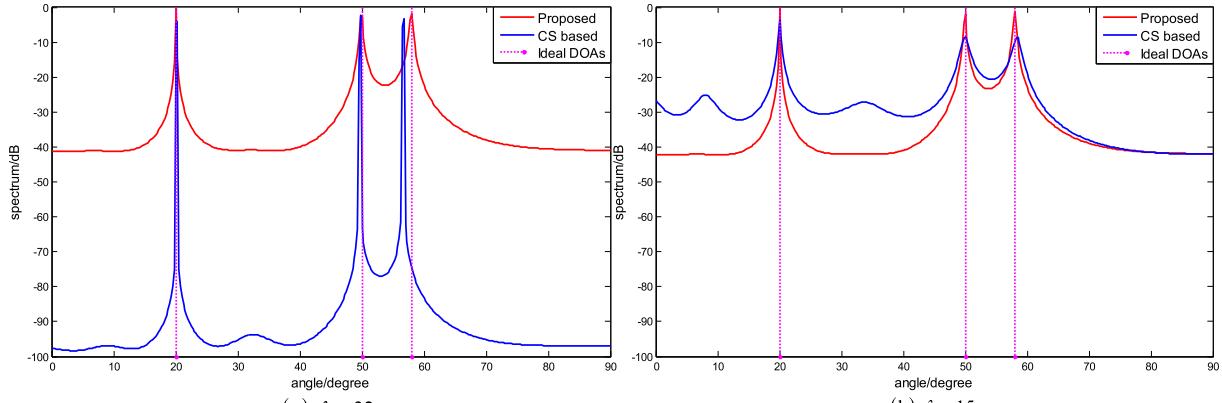

Fig. 6. Spatial spectra estimated for proposed method and CS-based method. (a) $\lambda_t = 32$, (b) $\lambda_t = 15$.

spatial smoothing based method. In many practical applications such as object detection in radar systems, torpedo detection in underwater sonar systems, it is of vital importance to realize fast detection, thus the proposed estimator possesses vast potentials in the future.

Acknowledgement

This work was supported by the National Natural Science Foundation of China under Grant 61671012, Qingdao National Laboratory for Marine Science and Technology under Grant No. QNLM2016OPR0411 and Applied Basic Research Plan of Qinghai (2017-ZJ-753).

Appendix A. Proof of the Proposition 1

Proof. (a) **Uniqueness**. For an integer $c \in [0, MN + M - 1]$, assume that there are two distinct integer pairs $(m, n), (m', n')$ such that $c = mN - nM$ and $c = m'N - n'M$ concurrently hold. Therefore, we have

$$\frac{M}{N} = \frac{m - m'}{n - n'}. \tag{A.1}$$

Since $m, m' \in [0, 2M - 1], n, n' \in [0, N - 1]$, (A.1) never holds due to the coprimality of M and N. In other words, $(m, n), (m', n')$ have to be the same integer pair and thus the uniqueness is proved.

(b) **Consecutiveness**. $\forall c \in [0, MN + M - 1]$, one can find a unique integer pair (m, n) such that $c = mN - nM$. Moreover, $0 \leqslant n \leqslant N - 1 \Longleftrightarrow 0 \leqslant nM \leqslant M(N - 1)$. Thus $0 \leqslant c + nM \leqslant 2MN - 1 \Rightarrow 0 \leqslant mN \leqslant 2MN - 1 \Rightarrow 0 \leqslant m \leqslant 2M - \frac{1}{N}$. Considering that m is an integer, thus we have $0 \leqslant m \leqslant 2M - 1$, which exactly accords with the expected range of m. Hence, the consecutiveness is proved.

References

[1] Zhang YD, Qin S, Amin MG. Doa estimation exploiting coprime arrays with sparse sensor spacing. In: IEEE international conference on acoustics, speech and signal processing. Springer; 2014. p. 2267–71.
[2] Cui K, Wu W, Huang J, Chen X, Yuan N. Doa estimation of lfm signals based on stft and multiple invariance esprit. AEU-Int J Electron Commun 2017;77:10–7.
[3] Pal P, Vaidyanathan PP. Nested arrays: a novel approach to array processing with enhanced degrees of freedom. IEEE Trans Signal Process 2010;58(8):4167–81.
[4] Liu CL, Vaidyanathan PP. Super nested arrays: linear sparse arrays with reduced mutual couplingpart. i: Fundamentals. IEEE Trans Signal Process 2016;64(15):3997–4012.
[5] Vaidyanathan PP. Sparse sensing with co-prime samplers and arrays. IEEE Trans Signal Process 2011;59(2):573–86.
[6] Pal P, Vaidyanathan PP. Coprime sampling and the music algorithm. In: Digital signal processing workshop and IEEE signal processing education workshop. Springer; 2011. p. 289–94.
[7] Qin S, Zhang YD, Amin MG. Generalized coprime array configurations for direction-of-arrival estimation. IEEE Trans Signal Process 2015;63(6):1377–90.
[8] Zhang YD, Amin MG, Himed B. Sparsity-based doa estimation using co-prime arrays. In: IEEE international conference on acoustics, speech and signal processing. Springer; 2013. p. 3967–71.
[9] Ye T, He X. Doa, power and polarization angle estimation using sparse signal reconstruction with a cold array. AEU - Int J Electron Commun 2015;69(11):1606–12.
[10] Wang X, Wang X, Lin X. Co-prime array processing with sum and difference co-array. In: 2015 49th Asilomar conference on signals, systems and computers. Springer; 2015. p. 380–4. https://doi.org/10.1109/ACSSC.2015.7421152.
[11] Li Y, Wang Y, Jiang T. Norm-adaption penalized least mean square/fourth algorithm for sparse channel estimation. Elsevier North-Holland, Inc.; 2016.
[12] Hoctor RT, Kassam SA. The unifying role of the coarray in aperture synthesis for coherent and incoherent imaging. Proc IEEE 1990;78(4):735–52. https://doi.org/10.1109/5.54811.
[13] Friedlander B, Weiss AJ. Direction finding using spatial smoothing with interpolated arrays. IEEE Trans Aerospace Electron Syst 1992;28(2):574–87. https://doi.org/10.1109/7.144583.
[14] Shan T-J, Wax M, Kailath T. On spatial smoothing for direction-of-arrival estimation of coherent signals. IEEE Trans Acoust Speech Signal Process 1985;33(4):806–11. https://doi.org/10.1109/TASSP.1985.1164649.
[15] Pillai SU, Kwon BH. Forward/backward spatial smoothing techniques for coherent signal identification. IEEE Trans Acoust Speech Signal Process 1989;37(1):8–15. https://doi.org/10.1109/29.17496.
[16] Schmidt R. Multiple emitter location and signal parameter estimation. Int J Eng Res 2013;2(3):276–80.
[17] Pan VY, Chen ZQ. The complexity of the matrix eigenproblem. In: ACM symposium on theory of computing, May 1–4, 1999, Atlanta, Georgia, USA; 1999. p. 507–16.
[18] Coppersmith D, Winograd S. Matrix multiplication via arithmetic progressions. J Symbol Comput 1990;9(3):251–80.